IOPscience

HOME | SEARCH | PACS & MSC | JOURNALS | ABOUT | CONTACT US

This article has been downloaded from IOPscience. Please scroll down to see the full text article.

(http://iopscience.iop.org/0268-1242/22/8/006)

More related content is available

Download details:
IP Address: 132.66.52.133
The article was downloaded on 29/01/2008 at 13:01

Please note that terms and conditions apply.

IOP Publishing Semiconductor Science and Technology

Semicond. Sci. Technol. **22** (2007) 863–869 doi:10.1088/0268-1242/22/8/006

Silicon heating by a microwave-drill applicator with optical thermometry

R Herskowits, P Livshits, S Stepanov, O Aktushev, S Ruschin and E Jerby

Faculty of Engineering, Tel Aviv University, Ramat Aviv 69978, Israel

E-mail: jerby@eng.tau.ac.il

Received 13 May 2006, in final form 30 May 2007
Published 29 June 2007
Online at stacks.iop.org/SST/22/863

Abstract
This paper presents a method for heating silicon wafers locally by open-end coaxial microwave applicators, with optical techniques employed for measuring the temperature. Silicon samples of $\sim 2 \times 2$ cm^2 area were radiated in air atmosphere by a microwave drill operating at 2.45 GHz in the range of 20–450 W. The rate of temperature variation was measured by the Fabry–Pérot etalon effect in samples illuminated by InGaAs lasers. The steady-state temperatures were measured by the changes in the absorption index of an InGaAs laser beam. The experimental results indicate heating rates of ~ 150 K s^{-1} and a temperature range of 300–900 K across the silicon sample during the microwave heating process. Further operation of the microwave drill caused local melting of the silicon samples. This paper presents the experimental setup and results, as well as numerical simulations of the microwave heating process.

(Some figures in this article are in colour only in the electronic version)

1. Introduction

Rapid thermal processes (RTPs) are applied to silicon wafers for oxidation, annealing, thin-film growing and other purposes [1–5]. RTP systems employ various heat-radiation sources [6] such as tungsten-halogen lamps. High-power microwaves ($\sim$3 MW pulsed) were used to melt silicon in the late 1980s [7]. Recent studies have introduced microwaves for silicon processes such as annealing, fast-firing and bonding [8–12]. The localized heating enabled by microwaves leads to new applications such as MEMS packaging, bonding and soldering [13–16].

This study is aimed at investigating the applicability of the microwave-drill device [17] as a means for local heating of silicon wafers. Optical techniques are used to measure the local temperature increase at various points across the silicon sample; hence the temperature measurements are conducted without interference to or from the microwave heating process.

2. Experimental setup

The experimental setup consists of a microwave apparatus for the silicon heating and an optical setup integrated with it to enable independent temperature measurement as described below.

2.1. The microwave apparatus

The microwave-drill apparatus employed for the silicon heating in this experiment is shown schematically in figure 1. It consists of a coaxial waveguide with a centre electrode of 1.6 mm diameter (140 Ω characteristic impedance). The microwave drill is fed by a 2.45 GHz power-adjusted magnetron (1.5 kW Alter SM-745) in a cascade with a circulator and an impedance-matching tuner, as shown in figure 2. The incident and reflected microwave power are detected by directional couplers.

A microwave power in the range of 20–450 W was applied locally to square pieces of 2×2 cm^2 silicon samples. Two kinds of N-type silicon samples were used, one was polished on both sides and the other was further coated by anti-reflective SiO layers ($\sim$375 nm thick on each side). The sample thickness was 0.37 mm or 1 mm for the polished samples, and 0.37 mm for the coated ones. The samples' resistivity was 5 Ω cm, except the 1 mm thick N-type sample with 100 Ω cm. The silicon sample was positioned in the chamber as shown

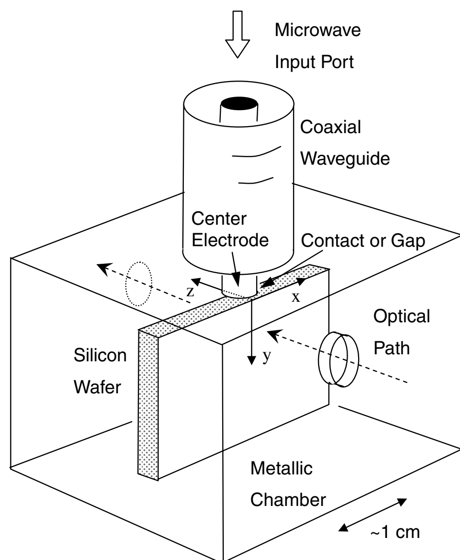

Figure 1. The microwave-drill apparatus for silicon-wafer heating. The device consists of a coaxial waveguide through which the microwave power is radiated to the wafer oriented along the coaxial-line centre electrode. The separated optical path perpendicular to the wafer enables non-interfering temperature measurements.

in figure 1. Experiments were conducted with the centre electrode in contact with the sample, or with a 1 mm gap between them.

The electrical conductivity of silicon at high temperatures approaches that of the metal; hence, its intrinsic impedance attains [18]

$$\eta(T) = \sqrt{j\frac{\mu_0\omega}{\sigma(T)}}, \tag{1}$$

where $\mu_0 = 4\pi \times 10^{-7}\ \Omega\ \mathrm{sm}^{-1}$ is the free-space permeability, ω is the microwave angular frequency and $\sigma(T)$ is the electrical conductivity given approximately by $\sigma(T) = 10^{4.247-2.924\times10^3\ T^{-1}}\Omega^{-1}\ \mathrm{m}^{-1}$, and T is temperature in K. The silicon impedance drops drastically as the temperature increases ($\eta < 1\ \Omega$ above 1273 K); hence the varying impedance-matching conditions are essential for efficient microwave-energy transfer to the sample. This effect is demonstrated by a numerical simulation of the microwave reflections from the device at various steady-state (uniform) temperatures. Figures 3(*a*) and (*b*) show the results obtained by the Ansoft-HFSS software (Version 9) for the microwave reflections from the coaxial waveguide in two different orientations of the silicon wafer. In figure 3(*a*) the silicon sample is oriented perpendicularly to the centre electrode (i.e., the sample is lying horizontally), whereas in figure 3(*b*) the sample is vertically on-axis with the centre electrode, as shown in figure 1. The silicon sample is 1 mm thick in these simulations at various doping levels. The results show that the microwave reflections in the on-axis orientation are considerably smaller; hence the microwave absorption is higher in this configuration than in the perpendicular orientation, and therefore it would be more effectively matched to enable a rapid heating. Yet,

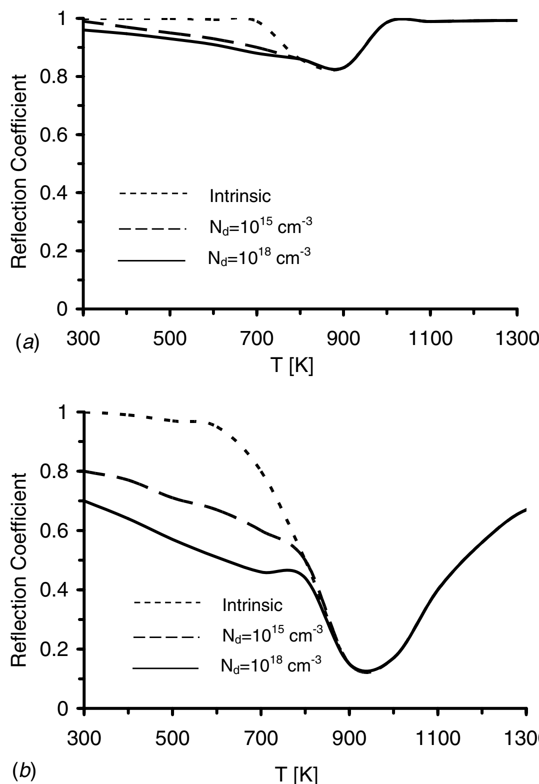

Figure 3. Numerical simulations of the reflection coefficient as a function of temperature for various doping levels in two different orientations of the silicon sample: (*a*) the silicon sample is lying horizontally in a perpendicular orientation to the centre electrode (in contact with its flat face), and (*b*) a vertical on-axis orientation, as shown in figure 1. These simulations were computed by Ansoft-HFSS (Version 9).

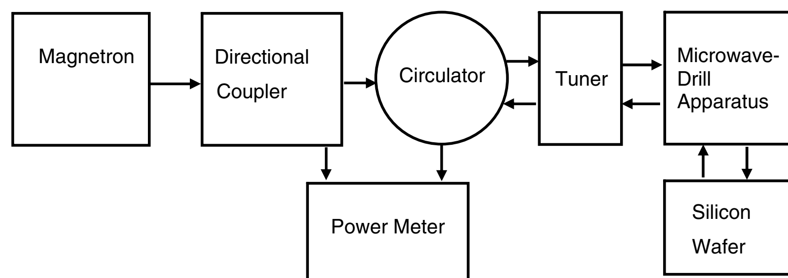

Figure 2. The microwave setup block diagram.

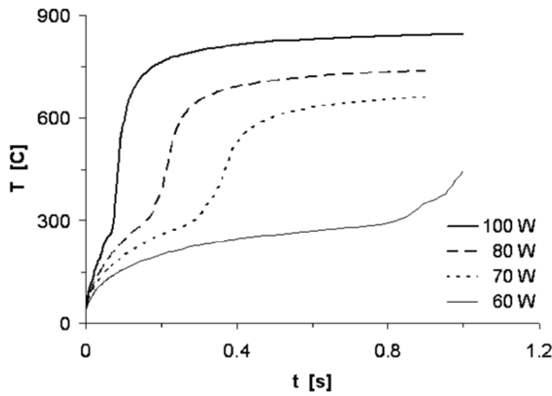

Figure 4. A numerical simulation of the temperature evolution in the silicon wafer in the configuration shown in figure 1 for various effective microwave power levels. The temperatures are given at a 1.5 mm distance from the wafer edge underneath the microwave centre electrode. This simulation employs the microwave-drill-coupled thermal-electromagnetic model [19].

the reflection coefficient depends strongly on the temperature. Furthermore, the microwave absorption increases significantly above 600 K, thus it may intensify the thermal runaway process there. Therefore, the microwave-drill-coupled thermal-electromagnetic model presented in [19] was employed to evaluate the heating rate in a simplified 2D approximation (assuming a silicon bulk instead of a wafer). Figure 4 shows the computed temperature evolution at a point 1.5 mm underneath the silicon upper (flat) face perpendicular to the central electrode. Local heating rates of several hundred K s^{-1} are predicted in these conditions.

2.2. *The optical setup*

The temperature measurement optical setup is shown in figure 5. It consists of two InGaAs laser diodes, operating at 1.3 μm, 1.5 μm wavelengths, and a collimator, filters and fast detectors. The InGaAs laser diodes were used to measure variations in the power transmitted through the heated silicon sample. The spot diameters of the lasers were ~1 mm. For each test, the temperature values were recorded during both the heating and the cooling phases of the sample. The measurements were verified independently by using two laser diodes at two different wavelengths, and by using two independent measurement techniques as described below.

An interferometric method based on a Fabry–Pérot etalon effect was employed to measure the variation in the refractive index of the polished silicon samples [20, 21]. This method enables one to estimate the temperature variation rate from the change in the refractive index due to the temperature-dependent lattice expansion and free-carrier generation [22]. The temperature-dependent refractive index of silicon in the range of 300–800 K can be approximated for near-infrared light by

$$n(T, \lambda) = n(T_0, \lambda) + A_n(T - T_0), \qquad (2)$$

where $T_0 = 300$ K, $n(T_0, \lambda) = 3.44$ and 3.47, for 1.5 μm and 1.3 μm wavelengths, respectively, and $A_n = 2 \times 10^{-4}$ at these wavelengths [23, 24]. Following Donnelly and McCaulley [20], the number of the interferometric light intensity oscillations due to the temperature change is

$$\Delta N(T) = \frac{2}{\lambda}[n(T, \lambda)h(T) - n(T_0, \lambda)h(T_0)], \qquad (3)$$

where $h(T)$ is the temperature-dependent thickness of the wafer.

Another aspect taken into consideration in these experiments is the variation in the silicon's absorption coefficient with temperature; hence the transmitted light is attenuated by

$$I_{\text{out}} = I_{\text{in}}\, e^{-\alpha(T)h(T)}, \qquad (4)$$

where I_{in} and I_{out} are the input and output light intensities, respectively, and $\alpha(T)$ is the temperature-dependent absorption coefficient given by Sturm and Reaves [25].

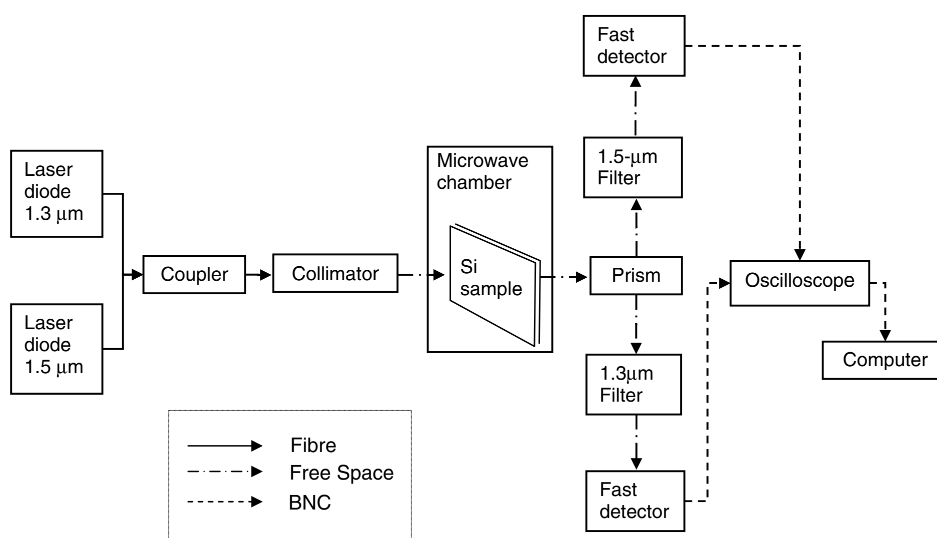

Figure 5. The optical setup for temperature measurements.

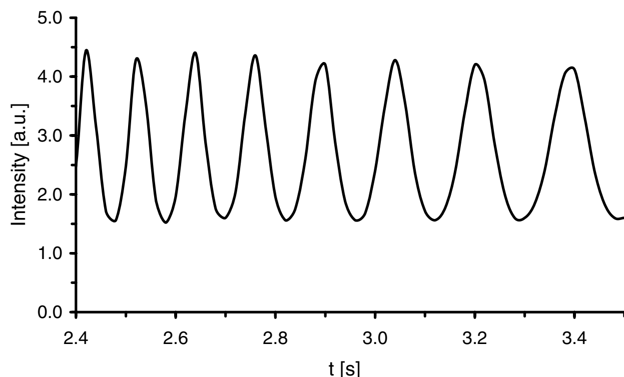

Figure 6. The light transmission intensity recorded in the Fabry–Pérot setup during the microwave heating experiment. The oscillations indicate the temperature variation rate according to equation (3).

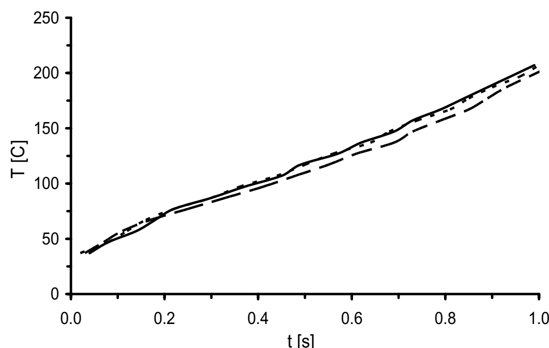

Figure 7. The temperature increase rate during the first second of the heating process of a polished silicon sample at 350 W with the centre electrode 1 mm apart from the samples. The measurements were done at three points across the sample, in the x, y coordinates (in mm): 0, 0 for the solid line, −6, 5 for the dashed line and 6, 5 for the doted line.

In the measurements performed on the double-sided polished samples, the light beams from the two InGaAs laser diodes were coupled together into a single beam which was then used to measure the temperature changes in the sample. Upon exiting the sample, the beam was separated by the corresponding filters into two beams, each targeted to a different detector. Hence, the same thermal phenomenon was measured redundantly by two independent wavelengths enabling validation of the results. For the measurements performed on the sample with the anti-reflective coating, we used the changes in the transmitted light intensity from the 1.5 μm wavelength laser diode.

3. Results

The temperature measurements described above were performed across the silicon sample at various microwave power levels, and in two positions of the central electrode with respect to the sample: one in physical contact and the other with a 1 mm gap between the two.

Figure 6 shows the oscillations in the transmission intensity through the Fabry–Pérot etalon due to the silicon heating. This measurement was performed on a polished sample using a 1.5 μm wavelength laser diode. According to equation (3), the calculated number of intensity cycles indicating a 100 K variation at $\lambda = 1.5$ μm is approximately 10, 13 and 27 for a sample thickness of 0.37 mm, 0.5 mm and 1 mm, respectively (the corresponding number of cycles at $\lambda = 1.3$ μm is 13, 17 and 34, respectively). From traces like figure 6, we extracted the temperature change rate $\Delta T(t)/\Delta t$ which was then integrated to find $T(t)$. The measurements were performed at several positions across each sample covering an area of $\sim 12 \times 5$ mm^2. The light source and the detector were moved accordingly in order to assure their alignment throughout the measurements. Figure 7 shows the temperature increase during the first second at three different positions across a silicon sample radiated by a 350 W source microwave power with the centre electrode 1 mm from the sample. The temperature increase rate is nearly the same near the heating point and at the two other points ~7 mm away from it on the sample.

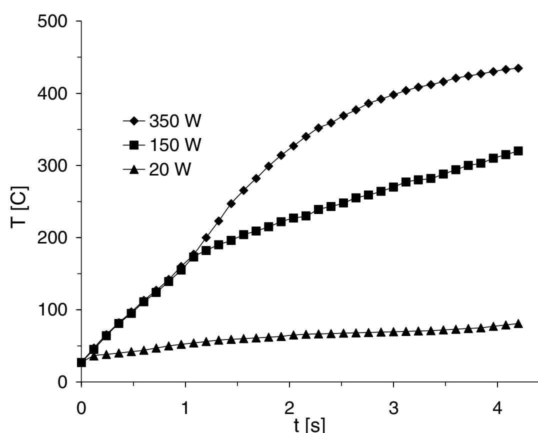

Figure 8. The temperature increase versus time for different microwave power levels applied to an N-type 370 μm thick silicon sample polished on both sides. The central electrode was 1 mm apart from the samples.

Figure 8 shows the temperature increase as a function of time for a 370 μm thickness N-type silicon polished sample at different values of the applied microwave power. In these experiments, the central electrode was fixed 1 mm above the sample; thus the temperature distribution is almost uniform across the sample. From the figure it can be seen that the temperature increase rate as well as the final temperature depends on the activated microwave power. Figure 9 shows the dependence of the heating rate on the silicon thickness for the same 350 W power applied. As expected, the heating rate is higher for thinner silicon samples.

The steady-state temperatures were also measured across a polished silicon sample irradiated by a 40 W microwave power conducted by a centre electrode which is in contact with the sample. Temperatures of 925 K near the contact point and 874 K ~7 mm away from it were measured. Hence, a temperature difference of about 50 K was observed. The results at a 100 W microwave power while the central electrode was located 1 mm away from the sample were 1050 K near the electrode and 1030 K at a distance of ~7 mm; hence, a temperature difference of only 20 K was seen between these two points (as seen also in figure 7). The temperature

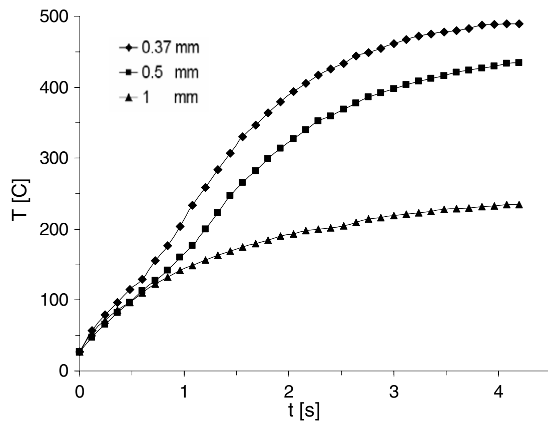

Figure 9. The temperature increase versus time for various silicon-wafer thicknesses at a 350 W microwave power. The central electrode was 1 mm apart from the samples.

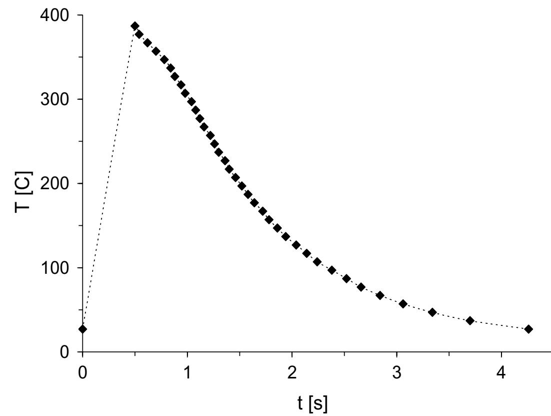

Figure 10. The temperature variation in time for a 370 μm thick N-type silicon wafer of a 5 Ω cm resistivity, in the case of plasma-assisted microwave heating for 0.5 s.

distribution is more uniform when the central electrode is at a distance of 1 mm from the sample rather than in direct contact with it.

During the performed measurements, we occasionally received a plasma effect. This was undesirable in this experiment since the light flash created by the plasma disturbed the optical measurements; hence, no measurements were performed during the heating processes, but only during the cooling processes. This allows only a partial evaluation and understanding of the phenomenon. Figure 10 shows the temperature cooling time for an N-type silicon sample at a 450 W microwave power. During this specific heating process, a plasma glow appeared for ~0.5 s which caused the temperature to increase much faster. A temperature of ~400 °C was reached after 0.5 s. As the plasma evolves the effective microwave power absorbed by it tends to increase significantly; hence more energy is absorbed also by the silicon. The excited plasma behaves in this case as a hot body transferring its heat energy to the silicon sample. The sample was subsequently examined by an optical microscope, but no damage or etches were observed. Similarly, 15 experiments were conducted with microwave plasma heating for N- and P-type silicon and the same results were obtained.

Figure 11 shows an optical image of a silicon sample with an anti-reflective coating after being exposed to microwaves for a longer time (>10 s). The centre electrode was in direct contact with the sample in this case. A small piece of the molten silicon can be seen; hence it is assumed that the temperature at the contact point exceeded 1685 K, the silicon's melting temperature. Away from the electrode's contact (the hottest point) the temperature decreases and the temperature distribution attains a semi-circular profile. It should be noted that the dissipated energy in the melting process was larger than the other heating experiments presented above at lower temperatures (in which no irreversible damage was caused to the silicon samples).

The heating process was simulated by a 3D thermal model based on [18]. A fixed power source (a hotspot) was assumed localized at the contact point of the microwave drill with the silicon wafer (i.e., at $x = y = 0$ in figure 1). The transient thermal model solves the heat equation with the convective and radiative boundary conditions, taking into account the time-dependent parameters of the silicon as given in [26, 27]. This simulation was performed using the Ansys Multi-Physics software (Version 10). For a qualitative comparison with the optical image shown in figure 11 this model was used to calculate the steady-state temperature profile for the centre electrode in direct contact with a 0.37 mm thick sample. The results are shown in figure 12(a) for a microwave power of 90 W and a silicon sample with anti-reflective coating. Similar circular equitemperature profiles, centred around the contact point of the centre electrode, can be seen in both images. The same simulation code was used to find the temporal changes in time of the temperature profile across the surface directly below the central electrode (at $y = 0$) as shown in figure 12, and the consequence spatial distribution of the temperature across the sample in the same conditions after 2 s.

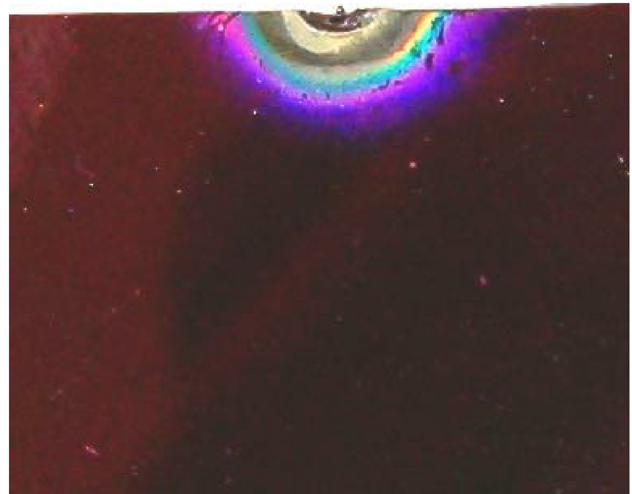

Figure 11. A silicon sample with an anti-reflective coating exposed to the microwave radiation. The high temperature profile evolved has left visible traces in the anti-reflective coating. A slight melting of the silicon is noticed in the contact point with the electrode.

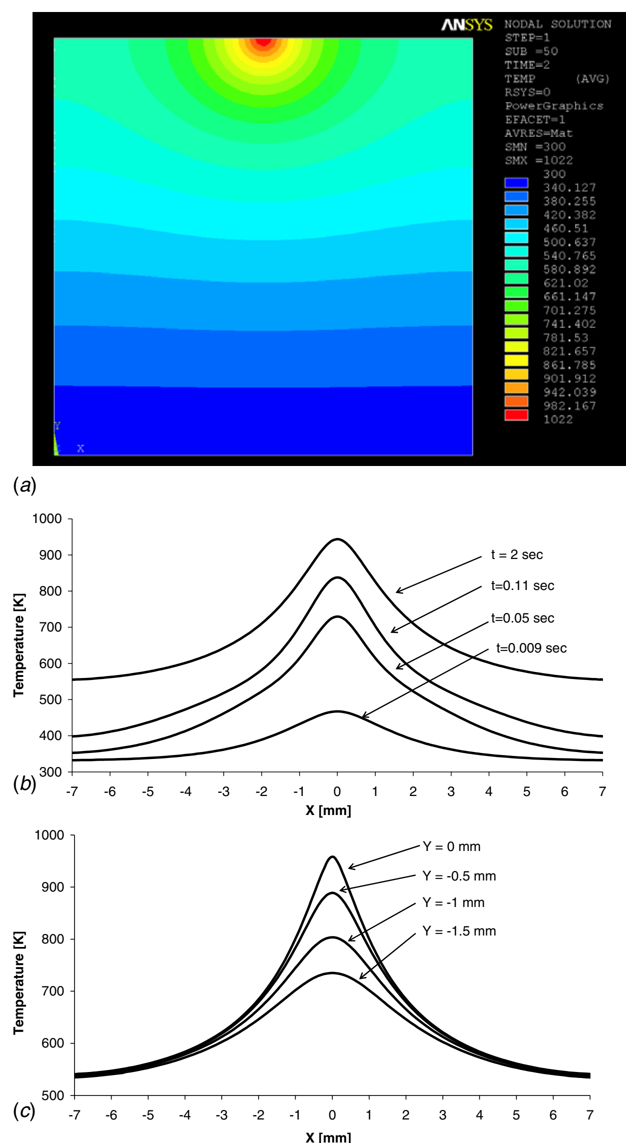

Figure 12. (*a*) The results of the Ansis simulation code performed for a microwave power of 90 W on a silicon sample with anti-reflective coating. (*b*) Changes in time of the temperature profile across the surface directly below the central electrode (at $y = 0$) obtained by the same simulation code, and (*c*) the spatial distribution of the temperature across the sample in the same conditions after 2 s.

4. Discussion

The various experiments presented above show that the microwave-drill concept provides a simple means for rapid heating of silicon wafers. The ability to control the heating rates and the final temperature, as well as the heating profile, stems from the optical thermometry incorporated in the microwave heating. As expected, the heating rate and the final temperature attained depend on the microwave power and on the wafer thickness. The centre electrode position, either in contact with the wafer or in some distance between them, affects the heating process as well.

The microwave drill is capable of generating local plasma when operating at higher energies. Hence, the plasma becomes the intermediate medium that absorbs the microwave power more effectively and heats up the wafer rapidly to the melting point (1685 K for silicon). This feature has been observed in our other melting, drilling and doping experiments [28]. The process of onset of such high temperatures locally deserves further investigation, in view of the known plasma applications for silicon heating (e.g. [29, 30]).

In future studies, the affected area could be determined by the microwave-drill dimensions, the geometry of radiated setup, and possibly by the number of radiating elements operated in an array. The temperatures can be controlled also by the microwave source power and duration. The temperature measurements method presented in this paper enables a real-time detection of the temperature evolved, with no interference with the microwave radiation. The heating process shall be simulated by a fully 3D coupled thermal-electromagnetic model, yet to be developed. The microwave-drill concept can be extended for various thermal processes in silicon [28] and even for local doping [31].

References

[1] Fiory A T 2002 Recent developments in rapid thermal processing *IEEE J. Electron. Mater.* **31** 981–7
See also Fiory A T 2005 Rapid thermal processing for silicon nanoelectronics applications *J. Minerals Metals Mater.* **57** 21–6

[2] Timans P J 1998 Rapid thermal processing technology for the 21st century *Mater. Sci. Semicond. Process.* **1** 169–79

[3] Kireev V Y and Tsimbalov A S 2001 Rapid thermal processing: a new step forward in microelectronics technologies *Russian Microelectron.* **30** 266–78

[4] Borisenko V 1997 *Rapid Thermal Processing of Semiconductors* (New York: Plenum)

[5] Tian C and Tujii F 2005 Nonlinear system identification of rapid thermal processing *Control Eng. Practice* **13** 681–7

[6] Hung S Y, Chao C K and Hsu C K 2005 Lamp design for fast cooling of rapid thermal processes with a two-zone lamp using a step cooling process *Semicond. Sci. Technol.* **20** 72–9

[7] James R B, Bolton P R, Alvarez R A, Christie W H and Valiga R E 1988 Melting of silicon by high-power pulsed microwave radiation *J. Appl. Phys.* **64** 3243–53

[8] Thompson K, Booske J H, Gianchandani Y B and Cooper R F 2002 Electromagnetic annealing for the 100 nm technology node *IEEE Electron. Devices Lett.* **23** 127–9

[9] Thompson K, Booske J H, Cooper R F and Gianchandani Y B 2003 Electromagnetic fast firing for ultra shallow junction formation *IEEE Trans. Semicond. Manuf.* **16** 460–8

[10] Bayrashev A and Ziaie B 2003 Silicon wafer bonding through RF dielectric heating *Sensors Actuators* A **103** 16–22

[11] Noh H, Moon K, Cannon A, Hesketh J and Wong C P 2004 Wafer bonding using microwave heating of parylene intermediate layers *J. Micromech. Microeng.* **14** 625–31

[12] Thompson K, Booske J H, Ives R L, Lohr J, Gorelov Y and Kajiwara K 2005 Millisecond microwave annealing: driving microelectronics nano *J. Vac. Sci. Technol.* B **23** 970–8

[13] Lin L 2000 MEMS post-packaging by localized heating and bonding *IEEE Trans. Adv. Packag.* **23** 608–16

[14] Cheng Y T, Lin L and Najafi K 2001 A hermetic glass-silicon package formed using localized aluminum/silicon-glass bonding *J. Microelectromech. Syst.* **10** 392–9

[15] Mescheder U M, Alavi M, Hiltmann K, Lietzau C, Nachtigall C and Sandmaier H 2002 Local laser bonding for low temperature budget *Sensors Actuators* A **97–98** 422–7

[16] Yang H A, Wu M and Fang W 2005 Localized induction heating solder bonding for wafer level MEMS packaging *J. Micromech. Microeng.* **15** 394–9

[17] Jerby E, Dikhtyar V, Aktushev O and Grosglick U 2002 The microwave drill *Science* **298** 587–9
[18] Thompson K, Gianchandani Y B, Booske J and F Cooper R 2002 Direct silicon-silicon bonding by electromagnetic induction heating *IEEE J. Microelectromech. Syst.* **11** 285–92
[19] Jerby E, Aktushev O and Dikhtyar V 2005 Theoretical analysis of the microwave-drill near-field localized heating effect *J. Appl. Phys.* **97** 034909
[20] Donnelly V M and McCaulley J A 1990 Infrared-laser interferometric thermometry: a nonintrusive technique for measuring semiconductor wafer temperatures *J. Vac. Sci. Technol.* A **8** 84–92
[21] Bond R A, Dzioba S and Naguib H M 1981 Temperature measurements of glass substrates during plasma etching *J. Vacuum Sci. Technol.* **18** 335–8
[22] Moss T S 1961 *Optical Properties of Semi-Conductors* (London: Butterworths)
[23] Lukes F 1959 The temperature-dependence of the refractive index of silicon *J. Phys. Chem. Solids* **11** 342–4
[24] Sato T 1967 Spectral emissivity of silicon *Japan. J. Appl. Phys.* **6** 339–47
[25] Sturm J C and Reaves C M 1992 Silicon temperature measurement by infrared absorption: fundamental processes and doping effects *IEEE Trans. Electron. Devices* **39** 81–8
[26] Timans P J 1993 Emissivity of silicon at elevated temperatures *J. Appl. Phys.* **74** 6353–64
[27] Asano A, Hsu P and Lojek B 2005 Temperature non-uniformity from combined conduction and radiation heat transfer within a doped wafer *RTP 2005: 13th Int. Conf. Adv. Thermal Processing of Semiconductors* p 239
[28] Livshits P, Dikhtyar V and Jerby E 2004 Localized heating, melting, and drilling of silicon *AIChE Annual Meeting*
[29] Hussein M G, Worhoff K, Sengo G and Driessen A 2007 Reduction of hydrogen-induced optical losses of plasma-enhanced chemical vapor deposition silicon oxynitride by phosphorus doping and heat treatment *J. Appl. Phys.* **101** 023517
[30] van den Donker M N, Schmitz R, Appenzeller W, Rech B, Kessels W M M and van de Sanden M C M 2006 The role of plasma induced substrate heating during high rate deposition of microcrystalline silicon solar cells *Thin Solid Films* **511–512** 562–6
[31] Jerby E, Livshits P, Dikhtyar V and Inberg A 2007 Silicon doping by a microwave-drill apparatus (to be published)